

Effects of the Hardened Nickel Coating on the Fatigue Behavior of CK45 Steel: Experimental, Finite Element Method, and Artificial Neural Network Modeling

E. Maleki* and K. Reza Kashyzadeh

* maleki_erfan@kish.sharif.edu

Received: June 2017

Accepted: November 2017

Mechanical Engineering Department, Sharif University of Technology, International Campus, Kish Island, Iran.

DOI: 10.22068/ijmse.14.4.81

Abstract: Hardened nickel coating is widely used in many industrial applications and manufacturing processes because of its benefits in improving the corrosion fatigue life. It is clear that increasing the coating thickness provides good protection against corrosion. However, it reduces the fatigue life. Thus, applying a thin layer of coated nickel might give an acceptable corrosion protection with minimum loss of the fatigue life. In the present study, the effects of hardened nickel coating with different thicknesses on the fatigue behavior of CK45 mild steel were experimentally investigated. After conducting the experimental tests, we carried out two different modeling approaches of finite element method (FEM) and artificial neural network (ANN). In the FEM modeling, an attempt was made to analyze the fatigue of the components by modeling the interface phase between the base metal and coating more accurately and using the spring elements; ANNs were developed based on the back propagation (BP) error algorithm. The comparison of the obtained results from FEM and ANN modeling with the experimental values indicates that both of the modeling approaches were tuned finely.

Keywords: Fatigue Test, Nickel Coating, Interface Phase, Finite Element Method, Artificial Neural Network.

1. INTRODUCTION

In many industrial and manufacturing applications, there exist many pieces of equipment subjected to repeated loads. Generally, fatigue fractures are the reason of 90 % of mechanical parts failure during their usage [1]. Likewise, some equipment components work in different environmental conditions such as dry, wet, and corrosive and the combination of corrosion and fatigue may cause the rapid failure of these components. On the other hand, damage caused by both corrosion and fatigue is more than the damage which is related to either fatigue or corrosion [1, 2]. Therefore, using beneficial approaches to obtain high levels of fatigue resistance and fine corrosion protection is considerable in different industries.

The effects of corrosive environments on the fatigue behavior of metals have been studied since 1930 [3]. Many methods have been employed to protect steel parts from corrosion and fatigue such as changing the stress of metal surface by shot peening, surface rolling, or

coating by organic or inorganic materials [4]. With respect to the cost and effectiveness, coating is the most common anti-corrosion treatment [3, 5]. Generally, electroplating (as one of the coatings methods) reduces the fatigue life of steel parts due to the initiation of micro cracks in the coating, which then penetrates through the substrate [6]. However, due to their useful effects, various coatings such as hardened chromium and nickel, warm galvanization, and titanium with different combinations (such as TiN, TiC, and TiO₂) are used in automotive, marine, and offshore structures and aerospace industries [6-9].

Many researchers have investigated the effects of different coatings on the mechanical properties and corrosion behavior of metallic materials [10-12]. However, only a few of them have investigated the coating influences on the fatigue behavior [13-16] related to the effect of coating thickness on the fatigue life of the different components [17-20].

In the present study, an attempt was made to study the effect of nickel coating thickness on the

fatigue life of CK45 steel by testing the fatigue experimentally. Afterwards, different modelling approaches of finite element method (FEM) and artificial neural network (ANN) were used to simulate the process. Three groups of standard specimens were prepared for the fatigue test, then the hardened nickel coatings were carried out to 26 specimens with various thicknesses of 13 and 19 μm and polishing performed on the other specimens.

The finite element models are widely used in different industries because of time and cost-saving. Therefore, many researchers in the area of coatings and their effects have focused on the different coatings of FEM and have performed fatigue analysis to predict the fatigue life and damage [5-7, 10-13]. The published results show that the fatigue life and fatigue strength of the coated samples were scientifically reduced in comparison with as-received ones [6, 21-22]. It is clear that the fatigue crack initiation and propagation normally start from the surface. However, the interface area between the base metal and the coating is a prone area for starting damage. Therefore, in the last decade, researchers have tried to simulate the real interface area by utilizing different methods such as spring connection, cohesive zone element, etc. [5-6]. The new connection pattern of spring is used to simulate the interface phase. The current model has been prepared based on the previous connection pattern of spring. The obtained results show that the present model is more accurate than the previous model in comparison with the fatigue test data.

On the other hand, ANNs are widely used as an alternative approach to tackle complex and ill-defined problems in different aspects of science and engineering [23]. Due to their massively parallel structure, ANN can deal with many multi-variables non-linear modeling for which an

accurate analytical solution is very difficult to obtain [24]. They can learn from examples, they are able to handle noisy and incomplete data, they are also able to deal with nonlinear problems [25].

Many researches have been able to successfully use ANN for modeling the fatigue behavior of the materials. Different ANN simulations are carried out for the fatigue life prediction of different materials such as composites [25-28], steels [29-31], and aluminums [32, 33]. Moreover, some studies have been conducted to model the other aspects of the fatigue behavior of materials such as fretting [34] and also the corrosion [35] fatigue behavior by using ANN. In present study, ANN modeling is developed using the data of the experimental tests, the stress amplitude and thickness of coating are regarded as the input parameters, and the fatigue life is considered as an output parameter of the network.

To the best of the authors' knowledge, this is the first study that investigates the capability of both FEM and ANN models in the simultaneous fatigue life prediction of the coated material. The comparison of the experimental results and the predicted values of both FEM and ANN are in good agreement and the modeling results are acceptable.

2. EXPERIMENTAL PROCEDURE

Three groups of standard specimens made of Ck45 steel with yield and ultimate stresses of 475 and 515 MPa were prepared for the rotating cantilever bending fatigue test according to the English standard BS3518 and Mac Adam Beam [7, 52]. Then, the hardened nickel coating was carried out to 26 specimens with various thicknesses of 13 and 19 μm in the same conditions of operation

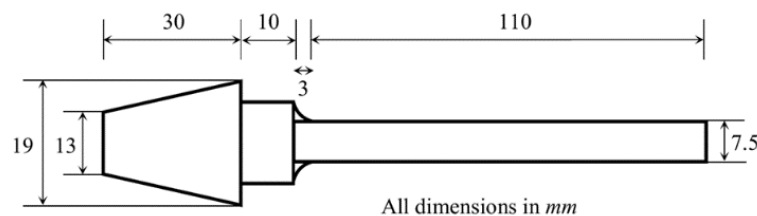


Fig. 1. Specimen dimensions for fatigue test

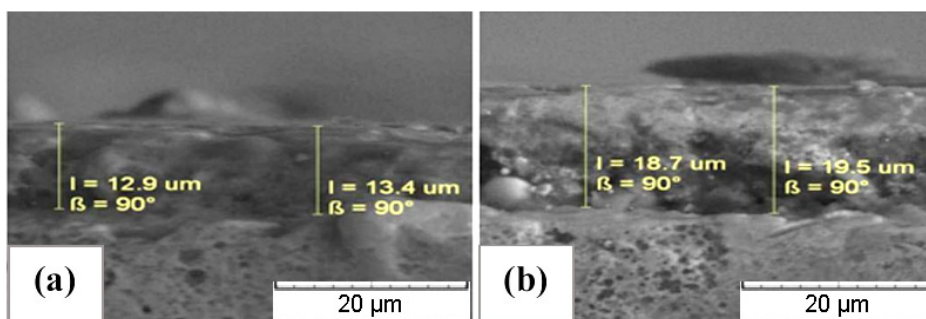


Fig. 2. Surface of components coating by SEM (a) Coating thickness is 13 μm (b) Coating thickness is 19 μm

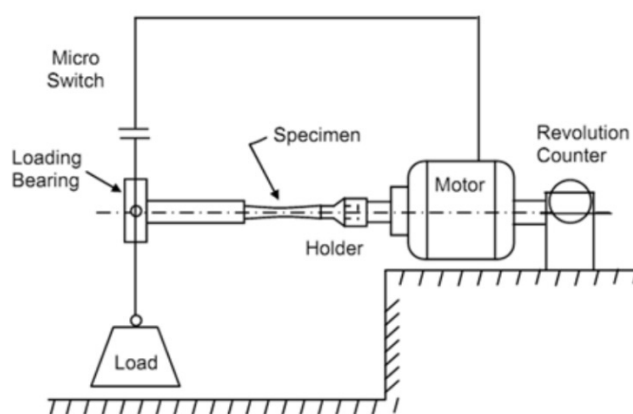


Fig. 3. Schematic of cantilever type rotating bending fatigue machine

including temperature, humidity, and other effective factors in the components [8, 9]. Polishing was performed on the other uncoated specimens. Figure 1 illustrates the dimensions of the used specimens in this study.

To analyze the accuracy of the plating and the thickness of the coatings, several Scanning Electronic Microscopy (SEM) images with different magnifications have been prepared as shown in Fig. 2.

The most common type of fatigue test, the rotating cantilever beam under pure bending load, was applied (see Fig. 3) such that the stress was always a reverse stress. The average stress is considered equal to zero and the stress ratio of $R = -1$ [4]. The loading frequency of 58 Hertz is used for all fatigue tests.

3. FINITE ELEMENT ANALYSIS

Full size of Mac Adam rotating cantilever beam under pure bending load was simulated by

using FEM. The geometrical dimensions and material are the same as those of the tested specimens (see Fig. 4). To create finite element simulation, three different types of mesh, including shell, solid, and linear spring, were used for coating, base metal, and interface phase, respectively. The mesh convergence was studied based on the previous FEM [6].

Two materials were used to investigate the fatigue life of the coated specimens as recommended by Vic [53]. The mechanical properties of the different components are presented in Table 1.

A thin hardened Nickel coating layer with the thicknesses of 13 and 19 μm was simulated on the base metal by assigning the related nickel mechanical characteristics to the finite element model.

The quality of the contact surface between the coating and base metal is the most important parameter on the simulation and response of the industrial coated parts.

In this model, 3D linear spring element is used

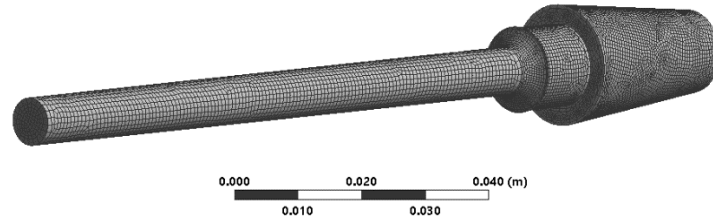


Fig. 4. Finite element model of the experimental specimen for the rotating cantilever bending beam

Table 1. Mechanical properties of the coated specimen components [53]

Component	Density [Kg/m ³]	Poisson's ratio	Elastic modulus [GPa]	Ultimate stress [MPa]	Yield stress [MPa]
Base Metal	7700	0.31	200	515	475
Coating	8890	0.315	220	1000	935

instead of Shell element in the previously simulated FEM [6], which has the axial, bending, and torsion stiffness. In the Model 1/4 of the components in the cylindrical coordinates, the number of nodes on the outer surface of the base metal is considered equal to the number of nodes on the interior surface of the coating; and the nodes of the two levels have been linked together with a certain connection pattern by utilizing the spring element. The spring stiffness (axial, bending, and torsion) of a solid cylindrical beam (base metal model) and a hollow cylindrical beam (coating) are obtained through resistance formulas, as we have [5]:

$$K_r = \frac{AE}{L^3} \quad (1)$$

$$K_\phi = \frac{JG}{L} \quad (2)$$

$$K_\theta = EI \quad (3)$$

One of the important parameters that must be considered in the present finite element model is the length of the spring element used to model the intermediate phase between the base metal and the coating. In order to specify the two side phases, the length of the metal link of the atoms of the two side phases is considered as the length of the circumference. In other words, it is considered equal to the length of the spring elements in the present model. We can see the finite element model used in

this research in Fig. 5:

Unit force is applied on the edge line of one end and the other end is fixed on 5 degrees of freedom (DOF) which can only rotate around the Z axis as boundary conditions. Constant angular velocity of 364.43 rad/s is applied on the FE model. Stress analysis is performed to determine the critical failure region. Then, the fatigue life of the specimens is predicted by utilizing the post-processing step of the finite element analysis output results in ANSYS-WORKBENCH software.

4. ARTIFICIAL NEURAL NETWORK

ANNs are computational models and their basis has been inspired by human's brain, which

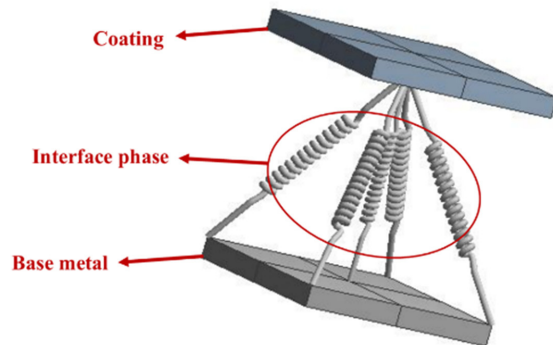


Fig. 5. A schematic of the new interface finite element model of the deposited components consisted of three independent phases

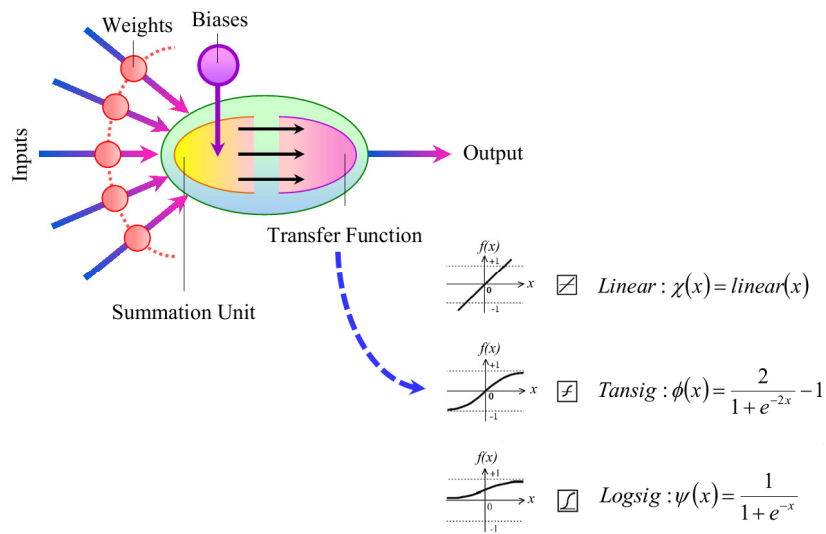


Fig. 6. Schematic of an artificial neuron

simulate the function of biological network composed of neurons. These networks have been widely employed to adapt and fit any complex database and have the power of prediction and optimization [36, 37]. The circumstance of modeling via ANN with considering the performance of the biological and artificial neurons has been researched in many studies [38, 39].

An artificial neuron is presented in Figure 6. A single neuron computes the sum of the entered inputs, which are multiplied with a variant called the weight, adds a bias term, and drives the result through a transfer function to produce a single output. Generally, linear, tangent sigmoid (Tansig), and logarithmic sigmoid (Logsig) functions are used as the popular transfer functions (see Fig. 6).

Structurally, every ANN is made up of input layer, hidden layer/layers, and output layer [40]. The structure of an ANN model is determined by the number of its layers, respective number of nodes in each layer, and the nature of the transfer function [41]. The architecture of a neural network that feeds with r and s input p and output a parameters respectively, with weight matrixes w , bias vectors b , linear combiner u , and transfer function f , is demonstrated in Figure 7.

4. 1. ANN Modeling

In order to model a process via ANN, two main

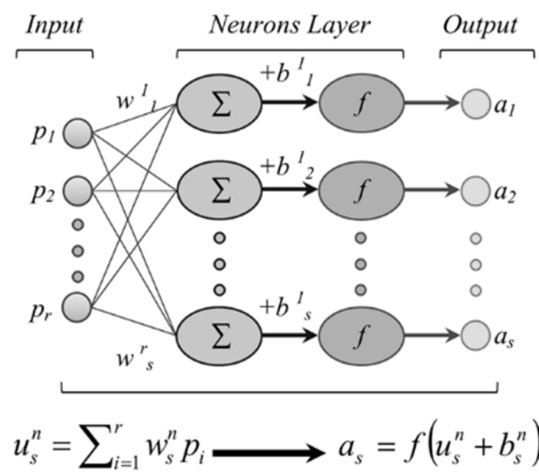


Fig. 7. One layer network that feeds inputs with r and outputs with s

steps of network training and testing must be considered. The main difference between these two networks is the used data sets; the employed data set for testing was not used during training. The training process is necessary to achieve the optimal network structure and the related parameters. However, the testing process is essential for performance assessment of the trained network. The scattering rate of the data must be regarded as the main point in developing the networks. In this study, all values of each

input and output data parameters are divided into maximum absolute value and then normalized; also the used data are dimensionless. The normalized data are in the range of [0, +1]. The used normalized data set for developing the networks is shown in Appendix A.

4. 2. Training and Testing Processes

Training is the process of determining the weights and biases values and obtaining the optimum patterns of learning. The sets of known data (inputs and outputs) are employed to train the network. However, there is no exact and suitable formula in order to obtain the optimal structure of ANN with the highest performance and accuracy and the least errors. Therefore, one of the challenging steps in ANN modeling is selecting the optimal architecture via trial and error [42, 43]. Usually, this procedure is accomplished by developing different networks with different structures. The developed networks are compared to gain the acceptable ranges of error. In this study, the feed-forward error back-propagation (BP) algorithm is used to train the networks. Although BP training algorithm has some drawbacks, this method was selected because of its simplicity and reliability. This algorithm is one of the most common and suitable ones for multilayer perceptions which minimize the error for particular training patterns

using the gradient descent technique [44].

In the present study, the fatigue behavior of non-coated and coated specimens of CK 45 steel with nickel coating was modeled. The amplitude stress and coating thickness are regarded as inputs and the number of cycles to failure is gathered as an output of the neural networks. Figure 8 displays the schematic of the ANN structure with four layers and feed-forward with BP algorithm in which all the neurons are fully interconnected.

The performance of the ANN modeling with regard to the effects of the hardened nickel coating on the fatigue behavior of CK45 mild alloy steel was evaluated using four statistical criteria, including: coefficient of correlation (R^2), root mean square error (RMSE), mean relative error (MRE), and mean absolute error (MAE). These statistical criteria have been determined as follows [51]:

$$R^2 = \frac{\sum_{i=1}^n (f_{EXP,i} - F_{EXP})(f_{ANN,i} - F_{ANN})}{\sqrt{\sum_{i=1}^n ((f_{EXP,i} - F_{EXP})^2 (f_{ANN,i} - F_{ANN})^2)}} \quad (4)$$

$$RMSE = \sqrt{\frac{\sum_{i=1}^n (f_{EXP,i} - f_{ANN,i})^2}{n}} \quad (5)$$

$$MRE = \frac{1}{n} \sum_{i=1}^n \left| \frac{f_{EXP,i} - f_{ANN,i}}{f_{EXP,i}} \right| \times 100 \quad (6)$$

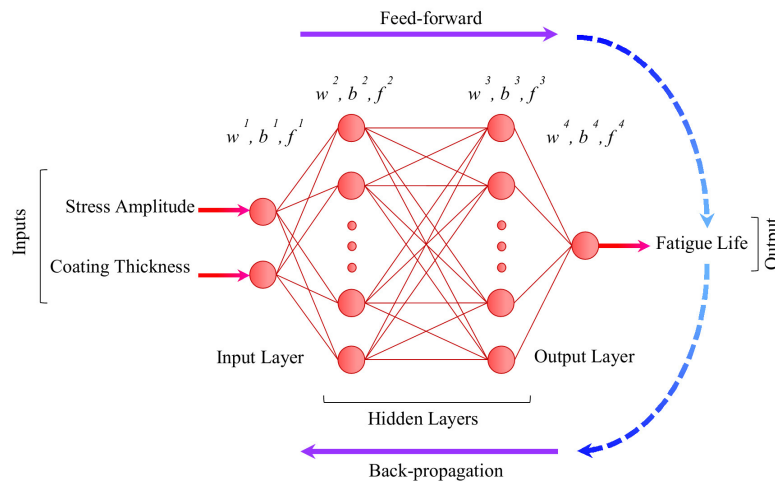


Fig. 8. Schematic of the ANN structure with four layers and feed-forward with BP algorithm

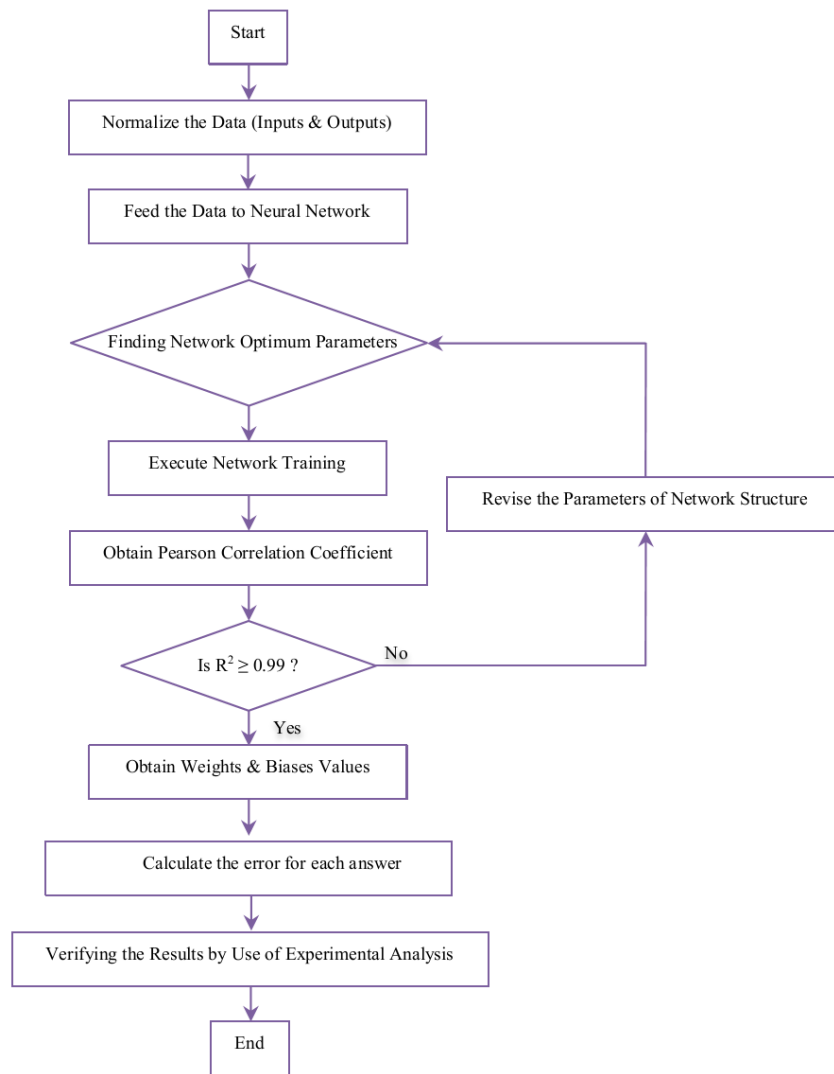


Fig. 9. The used methodology for developing ANN

$$MAE = \frac{1}{n} \sum_{i=1}^n |f_{EXP,i} - f_{ANN,i}| \quad (7)$$

where, n is the number of the used sample for modeling, f_{EXP} is the experimental value, and f_{ANN} is the networks' predicted value. Also, the values of F_{EXP} and F_{ANN} are calculated as follows [38]:

$$F_{EXP} = \frac{1}{n} \sum_{i=1}^n f_{EXP,i} \quad (8)$$

$$F_{ANN} = \frac{1}{n} \sum_{i=1}^n f_{ANN,i} \quad (9)$$

The methodology of ANN is stated due to the

convergence of errors criteria. The basis of the used method in this study is the value of R^2 , although the other values of statistical criteria such as RMSE [45] or mean square error (MSE) [46] can be employed as the foundation of the ANN developing approach. R^2 is a measure of correlation which is widely used as a rate of the degree of linear dependence between two variables. Based on the results reported by Elangovan et al. [47] and Maleki et al. [48-50, 54], R^2 values of more than 0.99 are much acceptable for this criterion. The methodology used for the neural network application is shown in Fig. 9.

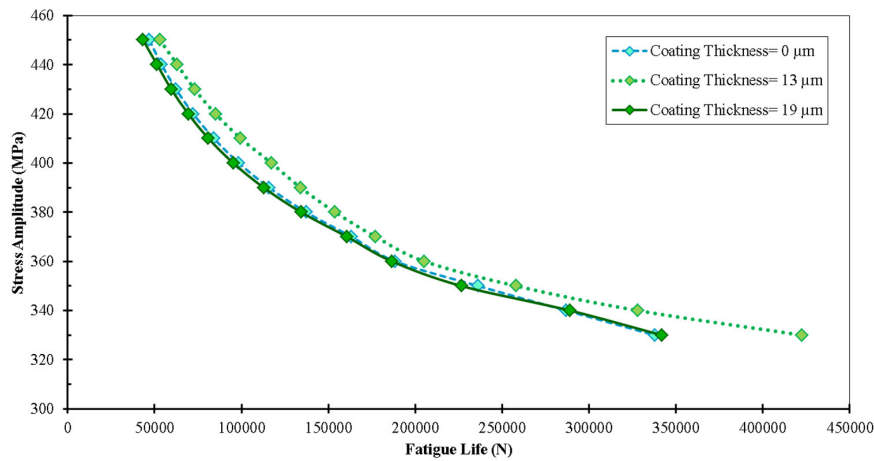


Fig. 10. S-N curve of the coated samples with different thickness

5. RESULTS AND DISCUSSION

5. 1. Experimental Results

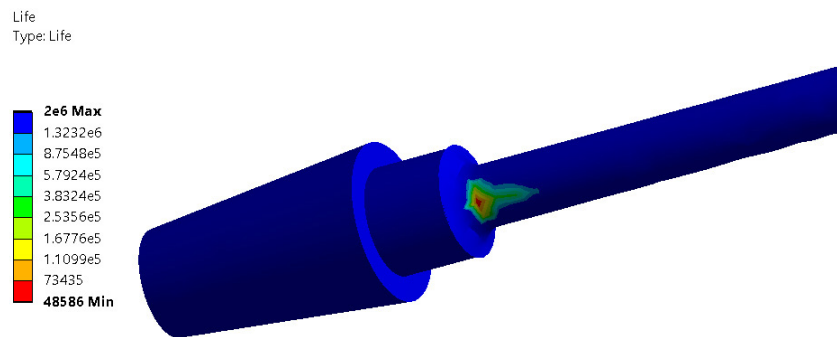
The fatigue test was performed for 13 different stress levels. The stress levels are selected lower than the yield stress to determine the fatigue life of the coated and uncoated specimens in the high cycle regime. The test was repeated twice for each level and the averages of the obtained results are reported as the failure cycle for each level of stress [4]. The fatigue test results are shown in Fig. 10.

According to the experimental results, it can be

observed that the highest range of the fatigue life is related to the coated specimens with thickness of 13 μm . Moreover, the fatigue life was reduced by increasing the thickness which had detrimental effects, and the lowest rate of the decreased fatigue life is for the coating thickness of 19 μm .

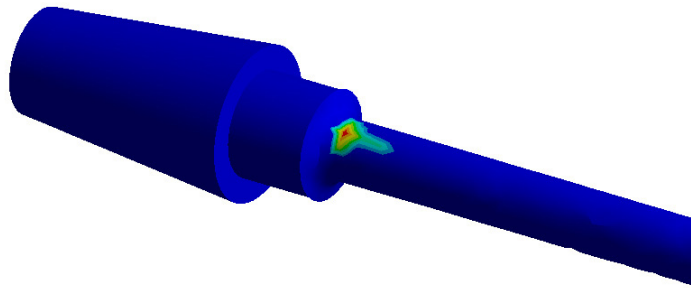
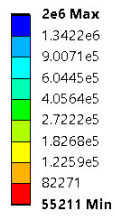
5. 2. FEM Results

After considering the requirements of the FEM simulation, the life contours of the specimens were achieved; the related results for the uncoated components are presented in Figure 11.



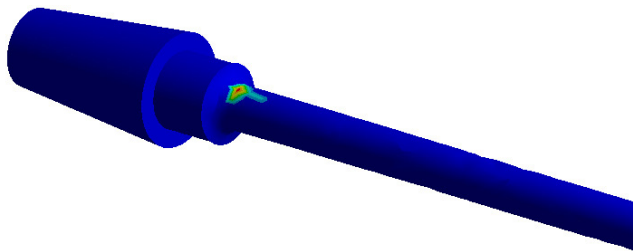
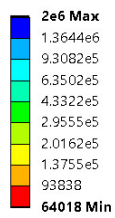
(a)

Life
Type: Life



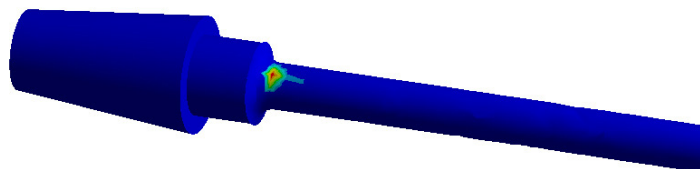
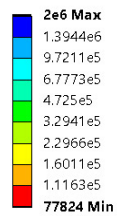
(b)

Life
Type: Life



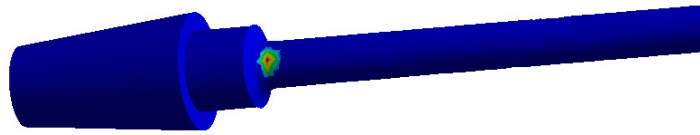
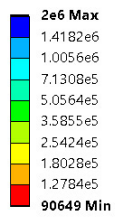
(c)

Life
Type: Life



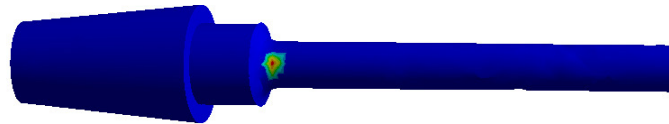
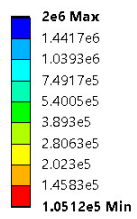
(d)

Life
Type: Life



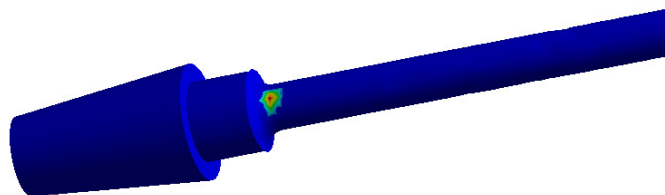
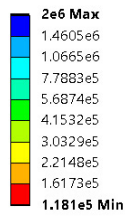
(e)

Life
Type: Life



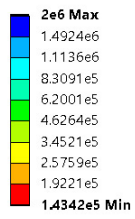
(f)

Life
Type: Life



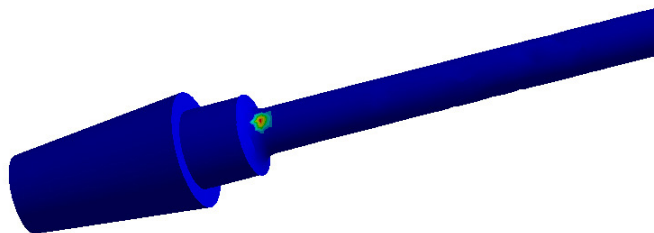
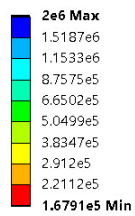
(g)

Life
Type: Life



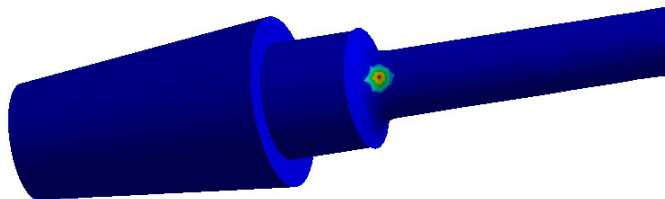
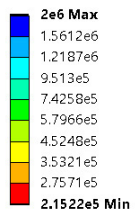
(h)

Life
Type: Life



(i)

Life
Type: Life



(j)

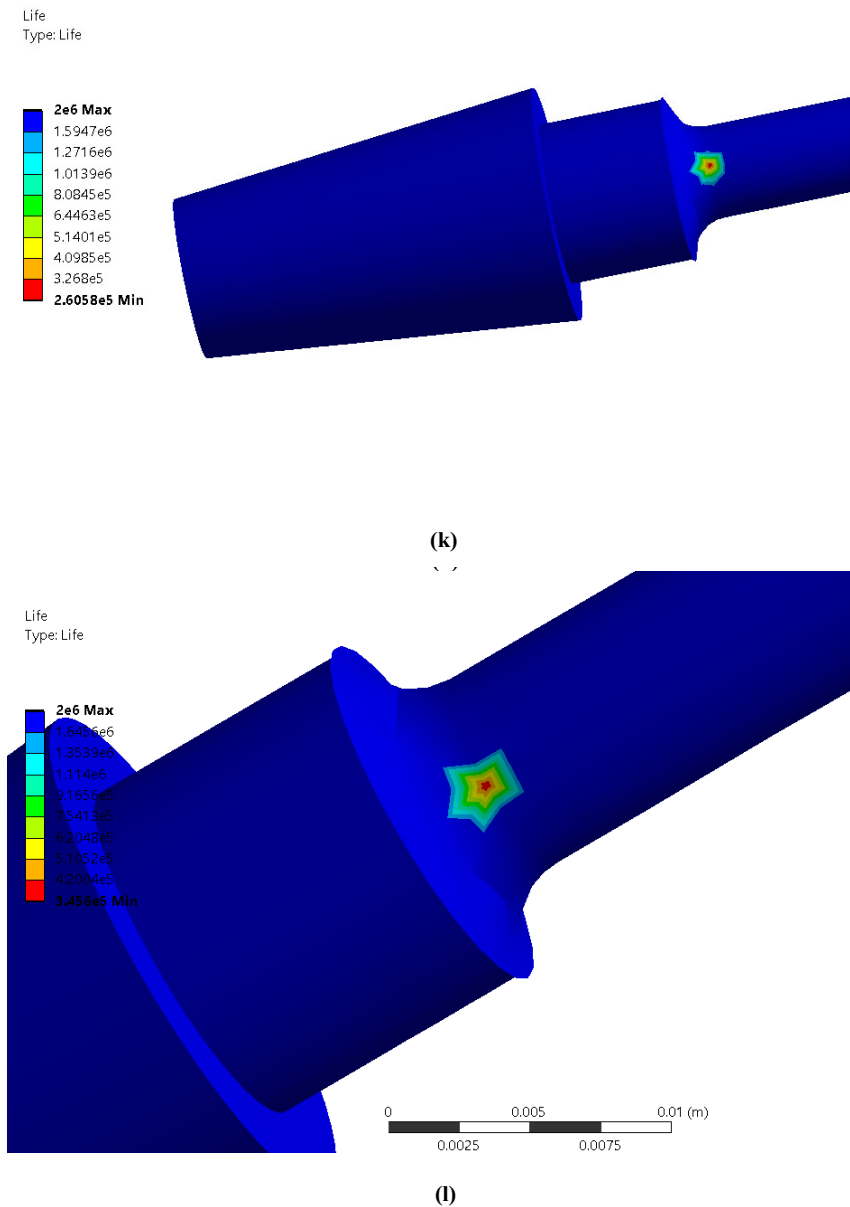


Fig. 11. The fatigue life contour for samples without coating under different stress levels: (a) Stress level of 440 MPa and failure cycle of 48586, (b) Stress level of 430 MPa and failure cycle of 55211, (c) Stress level of 420 MPa and failure cycle of 64018, (d) Stress level of 410 MPa and failure cycle of 77824, (e) Stress level of 400 MPa and failure cycle of 90649, (f) Stress level of 390 MPa and failure cycle of 105129, (g) Stress level of 380 MPa and failure cycle of 118116, (h) Stress level of 370 MPa and failure cycle of 143429, (i) Stress level of 360 MPa and failure cycle of 167910, (j) Stress level of 350 MPa and failure cycle of 215223, (k) Stress level of 340 MPa and failure cycle of 260587 and (l) Stress level of 330 MPa and failure cycle of 345647

There exists a small difference between the obtained results from the finite element analysis and the experimental data, which is negligible and acceptable. The main reason for this difference is using the linear spring element, which makes it possible to have a better

approximation to reality; the spring constants should also be calculated using the different theories of potential energy. However, in this research, the linear spring element has been employed to reach acceptable answers using the minimum amount of time (increasing the speed

of solving the equations) and simplification of ruling equations (using linear terms instead of nonlinear terms).

5. 3. ANN Results

Various networks were trained to achieve the optimal structure of the networks. The related information of 5 different trained networks with trial and error approach for modeling the fatigue life is shown in Table 2. As shown, the structure of the ANN modeling is stated from simple to complex; the more complexity of the networks structure, the higher rate of training will be to balance the speed of the training process. After investigating the trained network, the ANN modeling number 5 with the architecture of $2 \times 14 \times 14 \times 1$, which has the highest value of R^2

and the least values of RMSE, MRE, and MAE, is selected. Figure 12 shows the comparative diagrams of the predicted and experimental values for both the training and testing samples for all of the considered networks output parameters.

Based on the evaluation of the ANN via the mentioned statistical criteria for both the training and testing data sets, the relevant information of the employed network is shown in Table 3.

According to the obtained results, the values of R^2 in the network training are more than 0.999 and the RMSE, MRE, and MAE values are very close to zero. Thus, it is concluded that the networks are trained finely and adjusted carefully.

Likewise, the values of R^2 in the network testing are more than 0.999. The values of R^2 in

Table 2. The related information of 5 different networks for modeling the fatigue life of the coated CK45 steel

ANN Modeling No.	Rate of Training	Layers Structure	Hidden Transfer Function	Output Transfer Function	R^2	RMSE	MRE (%)	MAE
1	0.130	$2 \times 6 \times 8 \times 1$	Logsig	Linear	0.9868	0.0045	0.7293	0.0030
2	0.130	$2 \times 8 \times 10 \times 1$	Tansig	Linear	0.9889	0.0039	0.6774	0.0029
3	0.140	$2 \times 10 \times 12 \times 1$	Logsig	Logsig	0.9932	0.0034	0.6111	0.0023
4	0.145	$2 \times 12 \times 14 \times 1$	Logsig	Tansig	0.9987	0.0026	0.5688	0.0019
5	0.150	$2 \times 14 \times 14 \times 1$	Logsig	Logsig	0.9998	0.0022	0.5172	0.0016

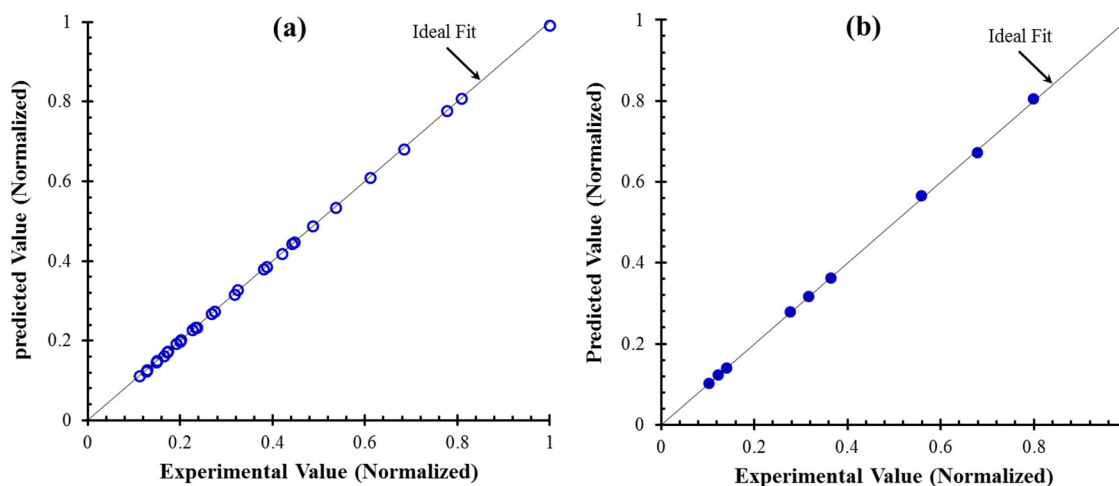


Fig. 12. The comparison of the ANN predicted and experimental values for each (a) training samples and (b) testing samples

Table 3. The obtained values of R^2 , RMSE, MRE, and MAE for the trained and tested network

Output parameter	Network Training				Network Testing			
	R^2	RMSE	MRE (%)	MAE	R^2	RMSE	MRE(%)	MAE
Fatigue Life	0.9999	0.0022	0.5172	0.0016	0.9997	0.0039	0.6693	0.0029

the networks testing have negligible reduction in comparison with the networks training. Moreover, the values of RMSE, MRE, and MAE in the networks testing are very small, which is acceptable. Totally, the results of the statistical criteria show that the obtained error values in the accomplished modeling is less than 1%.

5. 4. Comparison of the Experimental and Predicted Results

After accomplishing the simulations with two different approaches of FEM and ANN, their obtained results along with the achieved experimental values for each mentioned coating thicknesses of 0, 13, and 19 μm are separately illustrated in Figure 13.

Figure 14 depicts the obtained relative error (RE) values of both the FEM and ANN simulations for each considered amplitude stress and coating thickness. According to the results, the achieved minimum and maximum (min, max) values of RE for FEM and ANN are (min: 1.28, max: 14.20) and (min: 0, max: 1.430), respectively. Also, the FEM and ANN simulations have the average relative errors of 9.60 and 0.55 %, respectively. The achieved results indicate that in modeling the fatigue behavior of the nickel coated CK45 with different thicknesses, the ANN modeling has the lower error and more accuracy than the FEM simulation, although the carried out numerical solution is acceptable with considering the common and convectional ranges of errors for its related approach.

The point worth mentioning is that although the obtained results of ANN are more accurate than the FEM ones, if the used data set for developing the network changes, the new networks with different structures must be trained

and tested for predicting the fatigue life of the coated material. However, the accomplished FEM simulation, which is validated with the related experimental results, can be used in any other cases of coatings and base materials.

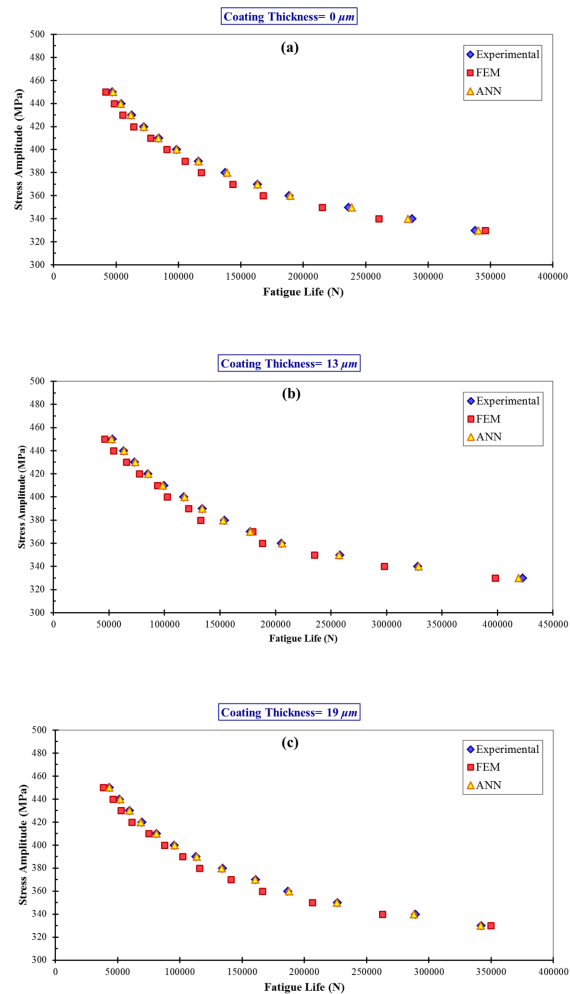


Fig. 13. The comparison of the experimental, FEM, and ANN results for (a) as-received, (b) coated with thickness of 13 μm , and (c) coated with thickness of 19 μm specimens

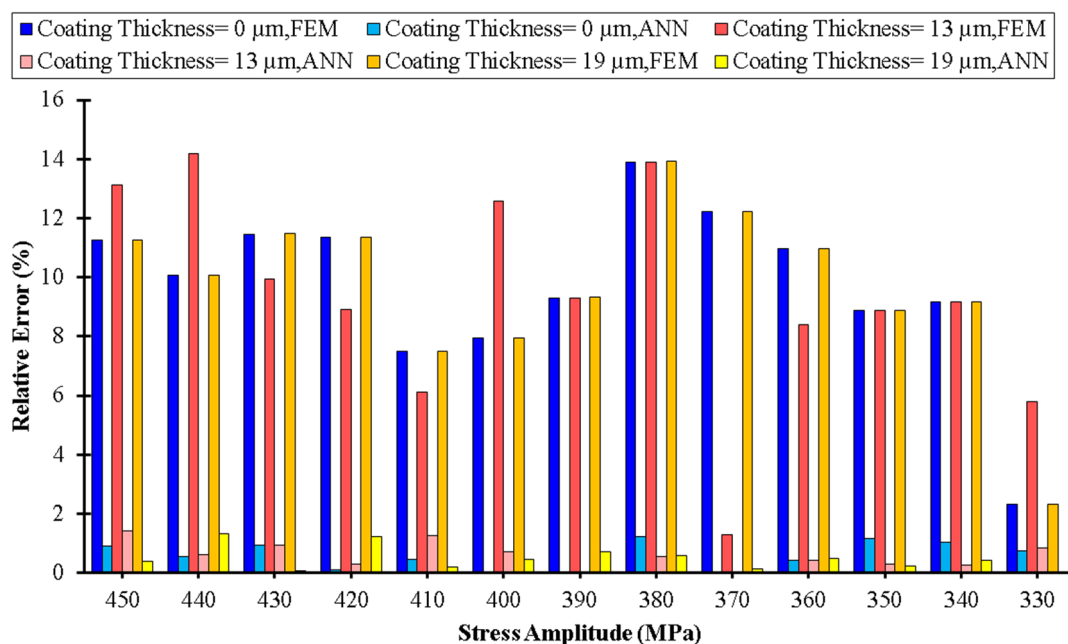


Fig. 14. The comparison of the obtained relative error values of the FEM and ANN results

Therefore, considering the advantages of the carried out simulations, when these methods are finely adjusted, the modeling results are in acceptable agreement with the experimental results. And both FEM and ANN can be used instead of experiments to decrease costs and the need for special testing facilities required to study the effects of coating thicknesses on the fatigue behavior of materials.

6. CONCLUSION

This paper studied the effect of the hardened nickel coating thickness on the fatigue life of CK45 steel with two different thicknesses. Performing the fatigue test resulted in the High-Cycle-Fatigue (HCF) properties of the coated samples with different thicknesses. Afterward, the capability of the two different approaches of FEM and ANN in modeling the fatigue life of the coated specimens was compared. The achieved results of the accomplished simulations represent that both simulations are acceptable and have good agreement with the experimental results and that both of them can be used instead of costly experiments. According to the obtained results,

FEM and ANN have the average relative errors of 9.60 and 0.55 %, respectively, and that the ANN model has a better performance than FEM. But, the presented neural network structures are unique to this case of base metal and coating. However, the accomplished FEM simulation, which is validated with the related experimental results, can be used in any other cases of coatings and base materials.

APPENDIX A.

Table A. The normalized data set for training and testing ANN

Sample No.	Thickness	Amplitude Stress	Fatigue Life Cycle	Sample Type
1	0	1.0000	0.1113	Training
2	0	0.9778	0.1279	
3	0	0.9556	0.1476	
4	0	0.9333	0.1709	
5	0	0.9111	0.1991	
6	0	0.8889	0.233	
7	0	0.8667	0.2743	
8	0	0.8444	0.3247	
9	0	0.8222	0.3867	
10	0	0.8000	0.4463	
11	0	0.7778	0.559	Testin د
12	0	0.7556	0.6791	
13	0	0.7333	0.7994	
14	0.6842	1.0000	0.1257	Training
15	0.6842	0.9778	0.1492	
16	0.6842	0.9556	0.1728	
17	0.6842	0.9333	0.2013	
18	0.6842	0.9111	0.2357	
19	0.6842	0.8889	0.2774	
20	0.6842	0.8667	0.3171	Testin د
21	0.6842	0.8444	0.3642	
22	0.6842	0.8222	0.4194	Training
23	0.6842	0.8000	0.4859	
24	0.6842	0.7778	0.6108	
25	0.6842	0.7556	0.7765	
26	0.6842	0.7333	1	
27	1	1.0000	0.1026	
28	1	0.9778	0.1217	
29	1	0.9556	0.1411	
30	1	0.9333	0.1642	Training
31	1	0.9111	0.1917	
32	1	0.8889	0.2256	
33	1	0.8667	0.267	
34	1	0.8444	0.3179	
35	1	0.8222	0.3805	
36	1	0.8000	0.4417	
37	1	0.7778	0.5363	
38	1	0.7556	0.6842	
39	1	0.7333	0.8091	

REFERENCE

- Zarras, P. and Stenger-Smith, J. D., “Corrosion processes and strategies for prevention: an introduction”, Part I, Handbook of Smart Coatings for Materials Protection, ed. A.S.H. Makhlof. Cambridge, England, 2014, 3-28.
- Forsgren, A., “Corrosion Control through Organic Coatings”, Taylor & Francis, London, England, 2006.
- Xin, L., “Anti-corrosion Coating and Coating Application”, Chemical Industry Press, Beijing, China, 2012.
- Lee, Y. L., Pan, J., Hathaway, R., Sarkey, M., “Fatigue Testing and Analysis: Theory and Practice”, Elsevier, Burlington, USA, 2005.
- Kashyzadeh, K. R. and Arghavan, A., “Study of the effect of different industrial coating with micro-scale thickness on the CK45 steel by experimental and finite element methods”, Strength of materials, 2013, 45, 748–757.
- Arghavan, A., Kashyzadeh, K. R. and Amiri

- Asfarjani, A., "Investigating effect of industrial coatings on fatigue damage", *Applied Mechanics and Materials*, 2011, 87, 230-237.
7. Ipaz, L., Caicedo, J. C., Esteve, J., Espinoza-Beltran, F. J. and Zambrano G., "Improvement of mechanical and tribological properties in steel surfaces by using Titanium–aluminum/titanium–aluminum nitride multilayered system", *Appl. Surf. Sci.*, 2012, 258, 3805-3814.
 8. Hay, J., "Mechanical Evaluation of Titanium-nitride-coated tool steel", Application Note, USA, 2010
 9. Krishna, D. S. R. and Sun, Y., "Thermally Oxidized Rutile-TiO₂ Coating on Stainless Steel for Tribological Properties and Corrosion Resistance Enhancement", *Appl. Surf. Sci.*, 2005, 252, 1107-1116.
 10. Ramírez, G., Jiménez-Piqué, E., Mestra, A., Vilaseca, M., Casellas, D. and Llanes, L., "A comparative study of the contact fatigue behavior and associated damage micromechanisms of TiN- and WC:H-coated cold-work tool steel", *Tribology International*, 2015, 88, 263-270
 11. Yang, X., Li, S. and Qi, H., "Effect of MCrAlY coating on the low-cycle fatigue behavior of a directionally solidified nickel-base superalloy at different temperatures", *Int. J. Fatigue*, 2015, 75, 126-134.
 12. Kovářík, O., Haušild, P., Čapek, J., Medřický, J., Siegl, J., Mušálek, R., Pala, Z., Curry, N. and Björklund, S., "Resonance bending fatigue testing with simultaneous damping measurement and its application on layered coatings", *Int. J. Fatigue*, 2016, 82, 300-309.
 13. Khatibi, G., Lederer, M., Betzwar Kotas, A., Frotscher, M., Krause, A. and Poehlmann, S., "High-cycle fatigue behavior of thin-walled CoCr tubes", *Int. J. Fatigue*, 2015, 80, 103-112.
 14. Mubarak, A., Akhter, P., Hamzah, E., Mohd Toff, M. R. H. and Qazi, I. A., "Effect of Coating Thickness on The Properties of TiN Coatings Deposited on Tool Steels using Cathodic Arc PVD Technique", *Surf. Rev. Lett.*, 2008, 15, 401-410.
 15. Colombo, D. A., Echeverría, M. D., Dommarco, R. C. and Massone, J. M., "Influence of TiN coating thickness on the rolling contact fatigue resistance of austempered ductile iron", *Wear*, 2016, 350-351, 82–88.
 16. Liu, H. K. and Wu, H. H., "Effect of silicon nitride coating thickness on fatigue of silicon microbeams", *Measurement*, 2014, 50, 1-9.
 17. Voorwald, H. J. C., Padilha, R. Q., Pigatin, L. W., Cioffi, M. O. H. and Silva, M. P., "Influence of electroless nickel interlayer thickness on fatigue strength of chromium plated AISI 4340 steel", *Proceeding of The 15 th European Conference of Fracture (ECF15)*, Stockholm, Sweden, 2004, 1-7.
 18. Al-Assaf, Y. and El Kadi, H., "Fatigue life prediction of composite materials using polynomial classifiers and recurrent neural networks", *Composite Structures*, 2007, 77, 561–569.
 19. Kalogirou, S. A., "Artificial intelligence for the modeling and control of combustion processes: A review", *Prog. Ene. Combu. Sci.*, 2003, 29, 515-566.
 20. Vassilopoulos, A. P., Georgopoulos, E. F. and Dionysopoulos, V., "Artificial neural networks in spectrum fatigue life prediction of composite materials", *Int. J. Fatigue*, 2007, 29, 20–29.
 21. Ortiz-Mancilla, M. J., Mariño-Berroterán, C., Berríos-Ortiz, J. A., Mesmacque, G. and Puchi-Cabrera, E. S., "Effect of a thin hard chromium coating on fatigue behaviour of 4140 steel", *Surface Engineering*, 2004, 20, 345-52.
 22. Baragetti, S. and Tordini, F., "A review of the fatigue behavior of components coated with thin hard corrosion resistant coatings", *The Open Corrosion Journal*, 2011, 4, 9-17.
 23. Azizi, A., Shafaei, S. and Rooki, R., "Wear rate prediction of grinding media using bpn and mlr models in grinding of sulphide ores", *IJMSE*, 2016, 13, 73-84.
 24. Shahbazi, B., Rezai, B., Chehreh Chelgani, S., Koleini, S. M. J. and Noaparast, M., "Estimation of gas holdup and input power in froth flotation using artificial neural network", *IJMSE*, 2015, 12, 12-19.
 25. Khoshjavan, S., Heidary, M. and Rezai, B., "Estimation of coal swelling index based on chemical properties of coal using artificial neural networks", *IJMSE*, 2010, 7, 1-11.
 26. Vassilopoulos, A. P., Georgopoulos, E. F. and Dionysopoulos, V., "Artificial neural networks in spectrum fatigue life prediction of composite

- materials”, *Int. J. Fatigue*, 2007, 29, 20–29.
27. Xiang, K. L., Xiang, P. Y. and Wu, Y. P., “Prediction of the fatigue life of natural rubber composites by artificial neural network approaches”, *Mater. Des.*, 2014, 57, 180–185.
 28. Lee, J. A., Almond, D. P. and Harris, B., “The use of neural networks for the prediction of fatigue lives of composite materials”, *Composites: Part A*, 1999, 30, 1159–1169.
 29. Gareth Pierce, S., Worden, K. and Bezazi, A., “Uncertainty analysis of a neural network used for fatigue lifetime prediction”, *Mechanical Systems and Signal Processing*, 2008, 22, 1395–1411.
 30. Kang, J. Y., Choi, B. I., Lee, H. J., Kim, J. S. and Kim, K. J., “Neural network application in fatigue damage analysis under multiaxial random loadings”, *Int. J. Fatigue*, 2006, 28, 132–140.
 31. Lotfi, B. and Beiss, P., “Application of neural networking for fatigue limit prediction of powder metallurgy steel parts”, *Mater. Des.*, 2013, 50, 440–44.
 32. Pujol, J. C. F. and Pinto, J. M. A., “A neural network approach to fatigue life prediction”, *Int. J. Fatigue*, 2011, 33, 313–322.
 33. Mishra, S. K., Brahma, A. and Dutta, K., “Low Cycle Fatigue Life Prediction of Al–Si–Mg Alloy Using Artificial Neural Network Approach”, *Trans. Indian Inst. Met.*, 2016, 69, 597–602.
 34. Orbanic, P. and Fajdiga, M., “A neural network approach to describing the fretting fatigue in aluminium–steel couplings”, *Int. J. Fatigue*, 2003, 25, 201–207.
 35. Cheng, Y., Huang, W. L., Zhou, C. Y., “Artificial neural network technology for the data processing of on-line corrosion fatigue crack growth monitoring”, *Int. J. Press. Vessels Pip.*, 1999, 76, 113–116.
 36. Genel, K., “Application of artificial neural network for predicting strain-life fatigue properties of steels on the basis of tensile tests”, *Int. J. Fatigue*, 2004, 26, 1027–1035.
 37. Maleki, N. and Maleki, E., “Modeling of Cathode Pt /C Electrolyte Degradation and Performance of a PEMFC using Artificial Neural Network”, *Proceedings of the The International Conference on Engineering & MIS 2015 (ICEMIS '15)*, Istanbul, Turkey, 2015, 1-8. doi: 10.1145/2832987.2833000
 38. Maleki, E. and Maleki, N., “artificial neural network modeling of pt/c cathode degradation in PEM fuel cell”, *J. Electron. Mater.*, 2016, 45, 3822–3834.
 39. Maleki, E. and Zabihollah, A., “Modeling of Shot Peening Effects on the Surface Properties of (TiB + TiC) / Ti–6Al–4V Composite Employing Artificial Neural Networks”, *MATERIALI IN TEHNOLOGIJE*, 2016, 50, 43–52.
 40. Jahanshahi, M., Maleki, E. and Ghiami, A., “On the efficiency of artificial neural networks for plastic analysis of planar frames in comparison with genetic algorithms and ant colony systems”, *Neural Comput. Appl.*, 2017, 28, 3209–3227.
 41. Zhao, J., Ding, H., Zhao, W., Huang, M., Wei, D. and Jiang, Z., “Modelling of the hot deformation behaviour of a titanium alloy using constitutive equations and artificial neural network”, *Comput. Mater. Sci.*, 2014, 92, 47–56.
 42. Esmailzadeh, M. and Aghaie-Khafri, M., “Finite element and artificial neural network analysis of ECAP”, *Comput. Mater. Sci.*, 2012, 63, 127–133.
 43. Maleki, E., Sadrhosseini, H. and Ghiami, A., “Investigation of Artificial Neural Networks Capability to Predict Viscosity of Lubricants Used in Journal Bearings”, *Proceedings of the The International Conference on Engineering & MIS 2015 (ICEMIS '15)*, Istanbul, Turkey, 2015, 1-7. doi: 10.1145/2832987.2833019
 44. Maleki, E. and Sherafatnia, K., “Investigation of single and dual step shot peening effects on mechanical and metallurgical properties of 18CrNiMo7-6 steel using artificial neural network”, *IJMMM*, 2016, 4, 100–105.
 45. Artrith, N., Urban, A., “An implementation of artificial neural-network potentials for atomistic materials simulations: Performance for TiO₂”, *Comput. Mater. Sci.*, 2016, 114, 135–150.
 46. Abendroth, M. and Kuna, M., “Determination of deformation and failure properties of ductile materials by means of the small punch test and neural networks”, *Comput. Mater. Sci.*, 2003, 28, 633–644.
 47. Elangovan, K., Narayanan, C. S. and Narayanasamy, R., “Modelling of forming limit

- diagram of perforated commercial pure aluminum sheets using artificial neural network”, *Comput. Mater. Sci.*, 2010, 47, 1072–1078.
48. Maleki, E., “Artificial neural networks application for modeling of friction stir welding effects on mechanical properties of 7075-T6 aluminum alloy”, *IOP Conference Series: Materials Science and Engineering*, 2015, 103, 012034. doi:10.1088/1757-899X/103/1/012034
 49. E. Maleki, G. H. Farrahi, K. Sherafatnia, “Application of Artificial Neural Network to Predict the Effects of Severe Shot Peening on Properties of Low Carbon Steel”, in: A. Öchsner and H. Altenbach (Eds.), *Machining, Joining and Modifications of Advanced Materials*, Springer, Singapore, 2016, 45-60.
 50. Maleki, E., “Modeling of Severe Shot Peening Effects to Obtain Nanocrystalline Surface on Cast Iron Using Artificial Neural Network”, *Materials Today: Proceedings*, 2016, 3, 2197–2206.
 51. Maleki, N., Kashanian, S., Maleki, E. and Nazari, M., “A Novel Enzyme Based Biosensor for Catechol Detection in Water Samples Using Artificial Neural Network”, *Biochemical Engineering Journal*, 2017, 128, 1-11.
 52. Tuckerman, L. B. and Aitchison, C. S., “Design of Specimens for Short-Time Fatigue Test”, *Technologic Papers of the Bureau of Standards*, 1924, 19, 47-55.
 53. Vic, P., “*IMMA Handbook of Engineering Materials*”, Institute of metals and materials Australasia, Melbourne, Australia, 1997.
 54. Kashyzadeh, R., K., Maleki, E., “Experimental Investigation and Artificial Neural Network Modeling of Warm Galvanization and Hardened Chromium Coatings Thickness Effects on Fatigue Life of AISI 1045 Carbon Steel”, *J. Fail. Anal. and Preven.*, 2017. doi.org /10.1007 /s11668-017-0362-8